Resonant ablation rules of femtosecond laser on Pr–Nd doped silicate glass

Zhi Luo (罗 志)[1], Ji'an Duan (段吉安)[1,*], Cong Wang (王 聪)[1], Xiaoyan Sun (孙小燕)[1], and Kai Yin (银 恺)[2]

[1]*State Key Laboratory of High Performance and Complex Manufacturing, Central South University, Changsha 410083, China*

[2]*Institute of Optics, University of Rochester, Rochester, NY 14627, USA*

[*]*Corresponding author: duanjian@csu.edu.cn*

Received February 3, 2015; accepted March 26, 2015; posted online April 20, 2015

Resonant effect is found in femtosecond laser ablating Pr–Nd glass. When processed with resonant wavelength of 807 nm, resonant ablation efficiency (RAE) with a single pulse can be improved by 45.22%. Furthermore, RAE closely relates to laser intensity. For resonant ablation, RAE is increased significantly when laser intensity $<0.556\times10^{14}$ W/cm^2 at which multiphoton ionization dominates, while it fades away when laser intensity $>0.556\times10^{14}$ W/cm^2 at which tunnel ionization dominates. Besides, it is also found that the ablation depth increases along with the wavelength rise when multiphoton ionization dominates, while the change rule is inversed when tunnel ionization dominates.

OCIS codes: 140.7090, 160.5690, 220.4000, 320.7110.

doi: 10.3788/COL201513.051403.

Femtosecond (fs) laser has many unique characteristics[1,2], e.g., it is flexible, nonpolluting, noncontacting, and has nonlinear absorption, which make it a promising tool for cross scale micro/nano-processing. However, the balance between quality and efficiency is still a bottleneck for the fs laser microfabrication[3,4]. At present, by adjusting the temporal and spatial intensity distribution to control the transient localized photon and electron dynamics, the efficiency of fs laser micro/nano-machining has been enhanced in some laboratories[5–7], but it is still not enough. In fact, besides optical field, physical properties of target materials, such as the bandgap of dielectrics, also have unneglectable effect on photon absorption and phase change of the materials, and they finally influence the quality and efficiency of fs laser fabricating[8–10]. In this work, we focus on researching the influence of different ionization mechanisms on efficiency of fs laser ablating one kind of special silicate glass whose absorption property has been changed by doping rare-earth elements praseodymium (Pr) and neodymium (Nd).

The initial and very important step of fs laser ablating dielectrics is converting bound electrons into free electrons, i.e., promoting the electrons from valance band to conduction band, which happens mainly through impact ionization and avalanche ionization. However, the seed electrons for these two kinds of ionization mechanisms are mostly produced by photoionization which includes multiphoton ionization and tunnel ionization[11]. Keldysh showed that the multiphoton ionization and tunnel ionization can coexist in the same process of fs laser–matter interaction, and the ratio depends on Keldysh parameter (γ) which is determined by laser intensity and ionization potential of target material. Multiphoton ionization dominates when $\gamma > 1$, while tunnel ionization dominates when $\gamma<1$[12,13]

$$\gamma = \frac{\omega}{e}\sqrt{2mI_P/I}, \tag{1}$$

$$I(x,y,z) = I_0\left(\frac{\omega_0}{\omega_z}\right)^2 \exp\left[-\frac{2(x^2+y^2)}{\omega_z^2}\right], \tag{2}$$

$$\omega_z = \omega_0\sqrt{1+\left(\frac{z\lambda}{\pi\omega_0^2}\right)^2}, \tag{3}$$

$$P = \int_0^{2\pi}\int_0^{+\infty} I_0\left(\frac{\omega_0}{\omega_z}\right)^2 \exp\left(-\frac{2r^2}{\omega_z^2}\right) r\mathrm{d}r\mathrm{d}\theta = \frac{\pi\omega_0^2 I_0}{2}, \tag{4}$$

where I_P is the ionization potential, I is the laser intensity, e is the electron charge, m is the electron mass, ω is the incident laser frequency, and $r = x^2 + y^2$. At any point in spatial intensity distribution, the laser intensity I can be calculated based on Eqs. (2)–(4).

As mentioned previously, the target material used in this work is Pr–Nd doped silicate glass (Pr–Nd glass; PNB586, China Jiangsu Hai'an Huihong Photoelectric Instrument Factory), whose selective absorption spectrum, measured with general weak light resource, is shown in Fig. 1. Because it is only from 700 to 810 nm that the laser has a fine fundamental transverse mode (TEM_{00} mode) of Gaussian distribution in our laboratory, 807 nm is selected as the resonant wavelength, which matches the energy gap between ground state $^4I_{9/2}$ and excited state $^4F_{5/2} + {}^2H_{9/2}$ of Nd^{3+} and whose absorption rate is 1.311. The photon energy of 807 nm is 1.536 eV and the bandgap of regular

 © 2015 Chinese Optics Letters

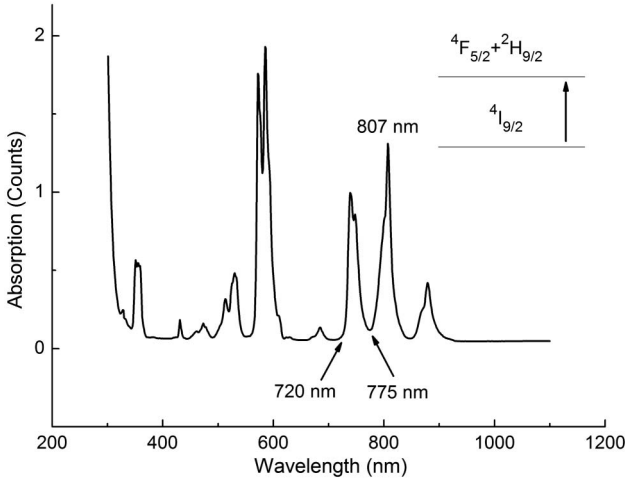

Fig. 1. Absorption spectrum of Pr–Nd glass. Resonant wavelength is 807 nm, whose absorption rate is 1.311. Nonresonant wavelengths are 775 and 720 nm, whose absorption rates are 0.118 and 0.066, respectively.

silicate glass is about 9 eV, so six photons should be absorbed simultaneously in order to ionize. Wavelengths of 775 and 720 nm are selected as nonresonant wavelengths, whose absorption rates are 0.1118 and 0.066, respectively. Six-photon ionization also occurs when irradiated by these two wavelengths. Besides, transparent fused silica is chosen as another target material for comparison, whose absorption spectrum is a horizontal line almost through zero in the wavelength range from 700 to 810 nm.

Figure 2 shows the schematic of the experiment setup. The laser source is a Ti:sapphire laser regenerative amplifier system (Spectra Physics), which provides a fundamental Gaussian beam with central wavelength of 800 nm, pulse duration of 120 fs, and repetition rate of 1 kHz. The laser wavelength can be tuned from 290 to 2600 nm through an optical parametric amplifier (OPA). After passing through a shutter, the laser energy is attenuated to 3 μJ/pulse by a pulse energy controlling unit which includes an attenuator, a half-wave plate, and a polarizer. Finally, the laser beam is focused into a tightly spot by an objective lens (Olympus, 20×, NA = 0.45). The measured waist radius is 1.50 μm, and laser energy is measured behind the objective lens. In order to monitor the fabrication process and the morphology of ablated microstructures, an observation system is built, which mainly consists of an illuminator to provide lighting and a charge-coupled device (CCD) to receive the reflected light from the sample, as shown in Fig. 2. After irradiation, confocal laser scanning microscope (CLSM; Zeiss LSM700) and atomic force microscope (AFM; Bruker Dimension Icon) are used to investigate the morphology.

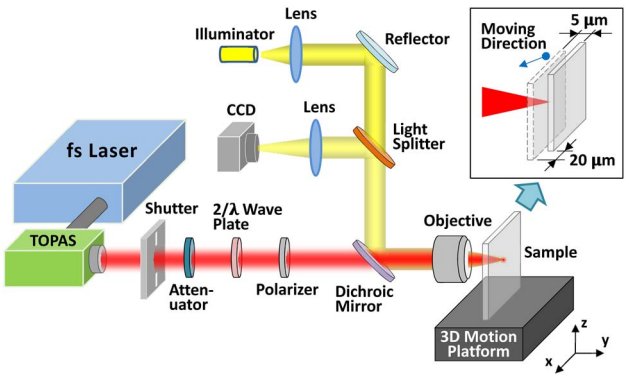

Fig. 2. Schematic of setup used for fs laser microprocessing.

As noted previously, laser intensity is one of the influential factors of ionization mechanism. In order to ablate Pr–Nd glass with different laser intensities, we can put the sample in different positions in the direction of laser propagation, because focused Gaussian beam will diverge behind beam waist and the central intensity will reduce gradually along with the beam propagation. Therefore, during processing, the sample first is placed far enough away from the focus (at least the surface cannot be damaged), then is translated close to the focus at a rate of 5 μm/step and moved 20 μm/step in the x-axis direction to separate micro-holes, as shown in Fig. 2, inset. All of these motions are performed with a high-precision 3D translation stage (XMS, Newport).

As the laser intensity weakens rapidly in the laser propagation direction, only one pulse is used in fabricating each micro-hole to keep laser intensity from reducing too much. Figure 3 shows micro-holes processed by the resonant wavelength of 807 nm and each hole is fabricated in a single illumination step with only one pulse. As the depth of micro-holes depends on the strongest laser intensity (SLI) at the central point of each pulse and laser intensity determines ionization mechanism, we choose to measure micro-holes' depths to reflect the ablation efficiency.

The measured depths of micro-holes, processed by fs laser with three selected wavelengths (720, 775, and 807 nm) on Pr–Nd glass and fused silica, are detailed in Fig. 4. The inflection point of each data curve indicates

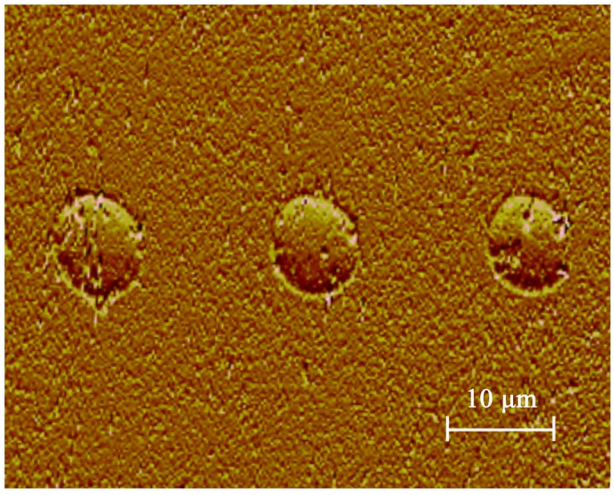

Fig. 3. AFM image of micro-holes fabricated by fs laser with resonant wavelength of 807 nm.

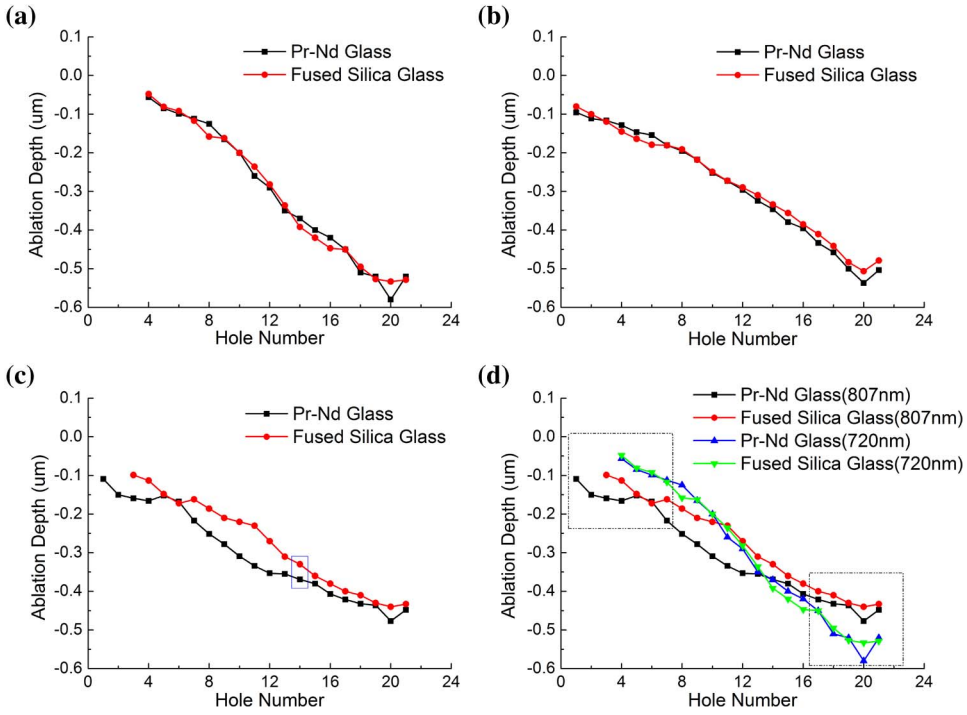

Fig. 4. Comparison of depths processed on Pr–Nd glass and fused silica by fs laser with a single pulse at different wavelengths: (a) 720 nm; (b) 775 nm; (c) 807 nm. (d) Overall contrast between 720 and 807 nm.

that the beam waist plane locates on the surface of sample at this point. And the farther away the data point is from the inflexion, the lower the corresponding laser intensity is. It can be seen from Fig. 4(c) that the two data curves separate obviously in the middle section, which means the efficiency is improved when ablating with resonant wavelength. However, processed with nonresonant wavelengths, the measured depths are almost equivalent to each other between on Pr–Nd glass and on fused silica, as shown in Figs. 4(a) and 4(b). That is because excited state lifetimes of rare-earth elements are very long, reaching up to several milliseconds (ms)[14], and the action time is just several fs between photons and electrons, as if only five photons were needed to excite multiphoton ionization for resonant wavelength 807 nm. The stable excited state just like an additional stair, which makes the resonant ionization easier compared with normal six-photon ionization. So far, it can be concluded that the ablation efficiency can be improved significantly when meeting resonant wavelength under a specific condition. In this work, the resonant ablation efficiency (RAE) is defined as

$$\eta = (H_{\mathrm{PN}} - H_{\mathrm{FS}})/H_{\mathrm{FS}} \times 100\% \tag{5}$$

where H_{PN} and H_{FS} are the measured depth of micro-holes processed on Pr–Nd glass and fused silica, respectively. The RAE is improved the most at the 11th micro-hole in Fig. 4(c), and it reaches 45.22%.

Relying on the calculation method mentioned previously, the SLIs corresponding to each micro-hole are calculated, as detailed in Fig. 5. The red circles represent

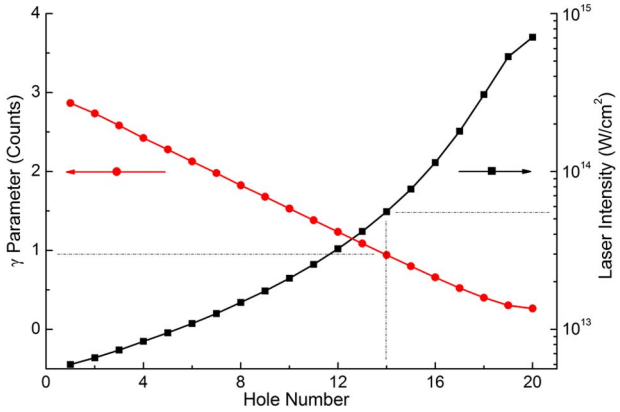

Fig. 5. SLI matching micro-holes processed by resonant wavelength of 807 nm and the corresponding Keldysh parameter γ.

Keldysh parameter γ. It is noted from Fig. 5 that the Keldysh parameter γ is 0.942($\approx$1) at 14th micro-hole, where the SLI is 0.556×10^{14} W/cm^2. Combined the theoretical analysis with experimental results in Fig. 4(c), it can be concluded that the multiphoton ionization dominates when laser intensity is lower than 0.556×10^{14} W/cm^2 while the tunnel ionization dominates when laser intensity is higher than 0.556×10^{14} W/cm^2, and RAE is only significant for multiphotion ionization. The RAE reaches maximum at the 11th micro-hole where the SLI is 0.258×10^{14} W/cm^2.

Compared the experimental results processed by 807 and 720 nm, as shown in Fig. 4(d), it can be found that the ablation depth with 807 nm is deeper than that with

720 nm during multiphoton ionization domination, while the relationship is inversed during tunnel ionization domination. Following the analysis in the previous section, the multiphoton ionization mainly depends on photon density. As photon energy of 720 and 807 nm are 1.722 and 1.536 eV, respectively, the photon density with 807 nm is almost 1.12 times than that with 720 nm at the illumination with equal laser energy. Therefore, the multiphoton ionization is easier for 807 nm. However, the tunnel ionization is chiefly determined by ponderomotive potential U_P ($U_P = e^2I/4m\omega^2$, referring to the quiver energy of an electron in electric field) and photon energy[15]. The ponderomotive potential of 720 nm is 42.906 eV which is almost equal to that of 807 nm with 43.017 eV, but the photon energy of 720 nm is 1.12 times than that of 807 nm, so the tunnel ionization is easier for 720 nm. All of these rules also work well with wavelength of 775 nm, which can be learned by comparing Figs. 4(b) and 4(d).

In conclusion, this work mainly studies the influence of different ionization mechanisms on efficiency of fs laser resonantly ablating Pr–Nd glass which owns special absorption spectrum. Three different wavelengths (720, 775, and 807 nm) are investigated, where only 807 nm is the resonant wavelength of Pr–Nd glass. When processed with resonant wavelength, the RAE is improved by up to 45.22%. While for nonresonant wavelength, the RAE almost fades away. Furthermore, RAE closely relates to laser intensity. When the laser intensity is less than 0.556×10^{14} W/cm^2 at which the multiphoton ionization dominates, RAE is increased obviously. When the laser intensity is higher than 0.556×10^{14} W/cm^2 at which the tunnel ionization dominates, RAE vanishes. Compared the experimental results processed with different wavelengths, it is found that the ablation depth increases along with the growth of wavelength when multiphoton ionization dominates. However, this change rule is inversed when tunnel ionization dominates.

This work was supported by the National "973" Program of China (No. 2011CB013000) and the National Natural Science Foundation of China (Nos. 91123035, 91323301, and 51335011).

References

1. B. N. Chichkov, C. Momma, S. Nolte, F. Von Alvensleben, and A. Tünnermann, Appl. Phys. A **63**, 109 (1996).
2. B. C. Stuart, M. D. Feit, S. Herman, A. M. Rubenchik, B. W. Shore, and M. D. Perry, Phys. Rev. B **53**, 1749 (1996).
3. K. O. Hill, B. Malo, F. Bilodeau, D. C. Johnson, and J. Albert, Appl. Phys. Lett. **62**, 1035 (1993).
4. A. Martinez, M. Dubov, I. Khrushchev, and I. Bennion, Electron. Lett. **40**, 1170 (2004).
5. C. Xu, L. Jiang, N. Leng, Y. Yuan, P. Liu, C. Wang, and Y. Lu, Chin. Opt. Lett. **11**, 041403 (2013).
6. B. Yalizay, T. Ersoy, B. Soylu, and S. Akturk, Appl. Phys. Lett. **100**, 031104 (2012).
7. L. Yang, A. El-Tamer, U. Hinze, J. Li, Y. Hu, W. Huang, J. Chu, and B. N. Chichkov, Appl. Phys. Lett. **105**, 041110 (2014).
8. X. Long, J. Bai, X. Liu, W. Zhao, and G. Cheng, Chin. Opt. Lett. **11**, 102301 (2013).
9. L. B. Fletcher, J. J. Witcher, N. Troy, S. T. Reis, R. K. Brow, and D. M. Krol, J. Appl. Phys. **112**, 023109 (2012).
10. J. Fang, L. Jiang, Q. Cao, Y. Yuan, L. Qu, J. A. Duan, and Y. Lu, Chin. Opt. Lett. **12**, 121402 (2014).
11. S. S. Mao, F. Quéré, S. Guizard, X. Mao, R. E. Russo, G. Petite, and P. Martin, Appl. Phys. A **79**, 1695 (2004).
12. L. V. Keldysh, Sov. Phys. JETP **20**, 1307 (1965).
13. T. Topcu and F. Robicheaux, Phys. Rev. A **86**, 053407 (2012).
14. N. Ohlsson, R. K. Mohan, and S. Kröll, Opt. Commun. **201**, 71 (2002).
15. B. F. Murphy, "Dynamics of noble gas cluster expansion driven by intense pulses of extreme ultraviolet light," Ph.D. Dissertation (University of Texas, 2009).